# Pancreatic islet amyloidosis, β-cell apoptosis, and α-cell proliferation are determinants of islet remodeling in type-2 diabetic baboons

Rodolfo Guardado-Mendoza[a], Alberto M. Davalli[b], Alberto O. Chavez[a], Gene B. Hubbard[c], Edward J. Dick[c], Abraham Majluf-Cruz[d], Carlos E. Tene-Perez[e], Lukasz Goldschmidt[f], John Hart[g], Carla Perego[h], Anthony G. Comuzzie[d], Maria Elizabeth Tejero[d], Giovanna Finzi[i], Claudia Placidi[i], Stefano La Rosa[i], Carlo Capella[i], Glenn Halff[j], Amalia Gastaldelli[a,k], Ralph A. DeFronzo[a], and Franco Folli[a,1]

[a]Department of Medicine Diabetes Division, University of Texas Health Science Center, San Antonio, TX 78229; [b]San Raffaele Scientific Institute, 20132 Milan, Italy; [c]Southwest Foundation for Biomedical Research and Southwest National Primate Research Center, San Antonio, TX 78227; [d]Unidad de Investigacion Medica en Trombosis y Aterogenesis, HGR #1 Gabriel Mancera, D.F. Mexico; [e]School of Medicine, University of Colima, C.P. 28040 Colima, Mexico; [f]Howard Hughes Medical Institute, University of California, Los Angeles–Department of Energy Institute of Genomics and Proteomics, Los Angeles, CA 90095-1570; [g]Department of Biochemistry, University of Texas Health Science Center and Department of Veterans Affairs Audie Murphy Division, Geriatric Research, Education, and Clinical Center, South Texas Veterans Health Care System, San Antonio, TX 78229; [h]Department of Molecular Sciences Applied to Biosystems, University of Milan, 20134 Milan, Italy; [i]Department of Pathology, Ospedale di Circolo, Department of Human Morphology, University of Insubria, and Centro Insubre di Biotecnologie per la Salute Umana, 21100 Varese, Italy; [j]Department of Surgery, University of Texas Health Science Center, San Antonio, TX 78229; and [k]Fondazione G. Monasterio and Institute of Clinical Physiology, National Research Council, 56126 Pisa, Italy

Communicated by C. Ronald Kahn, Harvard Medical School, Boston, MA, June 11, 2009 (received for review February 5, 2009)

**β-Cell dysfunction is an important factor in the development of hyperglycemia of type-2 diabetes mellitus, and pancreatic islet amyloidosis (IA) has been postulated to be one of the main contributors to impaired insulin secretion. The aim of this study was to evaluate the correlation of IA with metabolic parameters and its effect on islets of Langerhans remodeling and relative endocrine-cell volume in baboons. We sequenced the amylin peptide, determined the fibrillogenic propensities, and evaluated pancreatic histology, clinical and biochemical characteristics, and endocrine cell proliferation and apoptosis in 150 baboons with different metabolic status. Amylin sequence in the baboon was 92% similar to humans and showed superimposable fibrillogenic propensities. IA severity correlated with fasting plasma glucose (FPG) ($r = 0.662$, $P < 0.001$) and HbA1c ($r = 0.726$, $P < 0.001$), as well as with free fatty acid, glucagon values, decreased homeostasis model assessment (HOMA) insulin resistance, and HOMA-B. IA severity was associated with a decreased relative β-cell volume, and increased relative α-cell volume and hyperglucagonemia. These results strongly support the concept that IA and β-cell apoptosis in concert with α-cell proliferation and hypertrophy are key determinants of islets of Langerhans "dysfunctional remodeling" and hyperglycemia in the baboon, a nonhuman primate model of type-2 diabetes mellitus. The most important determinants of IA were age and FPG ($R^2 = 0.519$, $P < 0.0001$), and different FPG levels were sensitive and specific to predict IA severity. Finally, a predictive model for islet amyloid severity was generated with age and FPG as required variables.**

amyloid deposits | non-human primates | insulin resistance | islet of Langerhans | type-2 diabetes mellitus

Type-2 diabetes mellitus (T2DM) is a chronic metabolic disorder characterized by insulin resistance in liver, muscle, and adipose tissue, as well as progressive β-cell dysfunction leading to hyperglycemia (1–3). Hyperglycemia and islet amyloidosis (IA) have been implicated in the progressive loss of β cells in T2DM (4, 5). The prevalence of IA has been reported to range from 40 to 90% in T2DM individuals, and from 7% to 33% in nondiabetic controls (6–11). Islet amyloid pancreatic polypeptide (IAPP) is the major constituent of pancreatic amyloid deposits (12, 13). In humans, monkeys, and cats, but not in mice and rats, IAPP has an amyloidogenic-promoting region, which resides within amino acids 20 to 29. Abnormalities in IAPP processing and secretion have been proposed as important contributors to the formation of IA (14–17). Of note, IA and β-cell apoptosis have been observed in normal human islets transplanted into diabetic nude mice, as well as in the liver of type-1 diabetic patients transplanted with human islets (18, 19).

IA can cause β-cell death by occupying extracellular space, thereby impairing nutrients and oxygen uptake. In addition, small IAPP oligomers can form nonselective ion-permeable membrane pores, leading to increased intracellular calcium concentrations, endoplasmic reticulum stress, and apoptosis (20–25). However, one argument that has been raised against the pathogenic importance of IA in T2DM is that most, but not all pancreases contain amyloid deposits and only about 10% of patients with impaired fasting glucose have evidence of IA at postmortem (6, 7, 9, 10, 12, 13, 20).

Longitudinal studies in *Macaca nigra* and *Macaca mulatta* showed that progression to T2DM correlated with IA severity and that IA may play a role in β-cell death (26, 27). In this study, we performed a retrospective analysis in a large baboon (*Papio hamadryas*) population in which physical and clinical chemistry data, as well as pancreatic specimens, were available. Severe IA (> 50%) was not only associated with increased β-cell apoptosis and decreased relative β-cell volume but also with α-cell replication and hypertrophy and increased relative α-cell volume. In fact, α-cell proliferation correlated with hyperglucagonemia and hyperglycemia, providing new insights into the pathogenesis of islet of Langerhans "dysfunctional remodeling," and T2DM in the baboon.

## Results

**Sequencing and Fibrillogenic Propensity of Baboon IAPP.** Amyloid prevalence and amyloid severity had a hyperbolic relationship (Fig. S1*A*). Sequencing of the baboon IAPP gene showed a 90% identity to human IAPP at the cDNA level and 92% identity at the protein

Author contributions: R.G.-M., A.M.D., A.O.C., G.B.H., E.J.D., C.E.T.-P., C. Perego, A.G.C., G.F., C. Placidi, S.L.R., C.C., A.G., R.A.D., and F.F. designed research; R.G.-M., A.O.C., G.B.H., E.J.D., C. Perego, M.E.T., G.F., C. Placidi, S.L.R., C.C., G.H., and F.F. performed research; E.J.D., L.G., J.H., and C. Perego contributed new reagents/analytic tools; R.G.-M., A.M.D., A.O.C., G.B.H., A.M.-C., C.E.T.-P., L.G., J.H., A.G.C., M.E.T., G.F., C. Placidi, S.L.R., C.C., A.G., and F.F. analyzed data; and R.G.-M., A.M.D., A.O.C., A.M.-C., G.F., C. Placidi, S.L.R., C.C., A.G., and F.F. wrote the paper.

The authors declare no conflict of interest.

Freely available online through the PNAS open access option.

[1]To whom correspondence should be addressed. E-mail: folli@uthscsa.edu.

This article contains supporting information online at www.pnas.org/cgi/content/full/0906471106/DCSupplemental.

**Table 1. Physical and laboratory data of 150 baboons divided according to the severity of islet amyloid deposition (relative amyloid area)**

| Variable | Group 1 IA < 5.5% ($n$ = 30) | Group 2 IA 5.5–17% ($n$ = 30) | Group 3 IA 18–35% ($n$ = 30) | Group 4 IA 36–51% ($n$ = 30) | Group 5 IA > 51% ($n$ = 30) | $P$ group |
|---|---|---|---|---|---|---|
| Sex, (F/M) | 14/16 | 18/12 | 25/5[a,b] | 20/10 | 24/6[a,b] | 0.007 |
| Age, (years) | 16.2 ± 0.9 | 19.3 ± 0.8[a] | 19.8 ± 0.9[a] | 19.9 ± 0.9[a] | 21.6 ± 0.6[a] | 0.001 |
| Wt. (F, kg) | 15.7 ± 0.6 | 16.2 ± 0.8 | 15.8 ± 0.7 | 18.9 ± 1.2[c] | 21.4 ± 1.2[a,b,c] | 0.001 |
| Wt. (M, kg) | 30.2 ± 1.9 | 29.2 ± 1.5 | 29.6 ± 1.4 | 29.8 ± 2.0 | 30.7 ± 3.6 | 0.993 |
| FPG, (mg/dL) | 75 ± 2 | 83 ± 3 | 96 ± 7 | 115 ± 7[a,b] | 187 ± 21[a,b,c,d] | 0.001 |
| FFA, (mEq/L) | 0.53 ± 0.1 | 0.66 ± 0.1 | 0.6 ± 0.1 | 0.55 ± 0.08 | 1.15 ± 0.28[a,b,c,d] | 0.02 |
| Ins, ($\mu$IU/L) | 18 ± 4 | 18 ± 3 | 39 ± 17 | 40 ± 28 | 34 ± 11 | 0.724 |
| Glucagon, (pg/mL) | 60 ± 5 | 79 ± 10 | 97 ± 14 | 96 ± 20 | 112 ± 23[a] | 0.023 |
| HbA1c, (%) | 4.6 ± 0.2 | 4.9 ± 0.4 | 6.0 ± 0.7 | 6.5 ± 1.3 | 9.3 ± 0.9[a,b,c,d] | 0.004 |

FFA, free fatty acid; FPG, fasting plasma glucose; IA, islet amyloidosis.
[a]$P < 0.05$ vs. Group 1.
[b]$P < 0.05$ vs. Group 2.
[c]$P < 0.05$ vs. Group 3.
[d]$P < 0.05$ vs. Group 4.

level (Fig. S1*B*), and the fibrillation propensities of baboon and human IAPP were superimposable (Fig. S1 *C* and *D*).

**Morphometric, Physical, and Biochemical Data.** Physical and laboratory data are summarized in Table 1. Age, body weight in females, fasting plasma glucose (FPG), HbA1c, free fatty acid (FFA), and glucagon progressively increased with IA. In contrast, insulin levels did not differ significantly in the 5 groups. Morphometric data are summarized in Table S1. The baboon population was divided into quintiles according to IA. Mean islet size, relative islet volume, islet density, and relative amyloid volume (percentage of total pancreas occupied by amyloid) were increased according to IA severity ($P < 0.05$).

**$\beta$-Cell Function and Insulin Resistance.** $\beta$-Cell function [homeostasis model assessment (HOMA)-B] decreased progressively with increasing IA ($r = -0.509$, $P < 0.001$) (Fig. 1*A*) and FPG levels ($r = -0.589$, $P < 0.001$) (Fig. 1*B*). Insulin resistance (HOMA-IR) directly correlated with IA severity ($r = 0.217$, p 0.010) (Fig. 1*C*), and with FPG levels ($r = 0.292$, $P < 0.001$) (Fig. 1*D*). Of note, $\beta$-cell function decreased dramatically because of the additive effect of hyperglycemia (FPG >115 mg/dL) and IA severity (Fig. 1*E*).

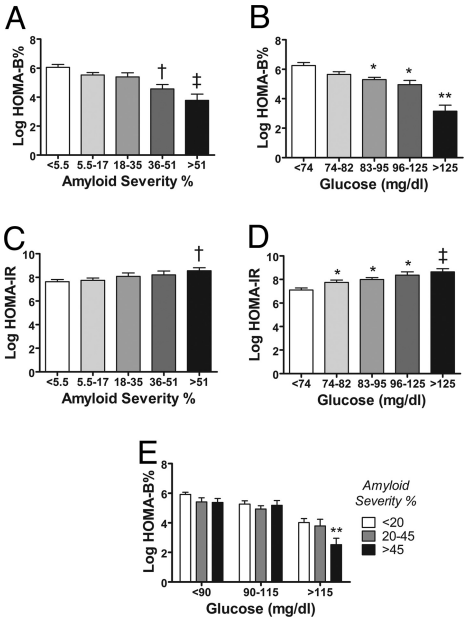


**Fig. 1.** $\beta$-Cell function and insulin resistance correlated with amyloid deposits and FPG in baboons. Ln(HOMA-B) (*A* and *B*) and Ln(HOMA-IR) (*C* and *D*) are depicted according to amyloid severity (IA) and FPG concentration in baboons. (*E*) Effect of increasing FPG concentration and worsening severity of amyloid deposition on $\beta$-cell function (ln HOMA B) in baboons. *, $P < 0.05$ vs. Group 1; †, $P < 0.05$ vs. Group 1 and 2; ‡, $P < 0.05$ vs. Groups 1, 2 and 3; **, $P < 0.05$ vs. all groups.

**Relationship Between IA Severity, FPG Levels, and Other Metabolic Parameters.** Weight and FPG distribution in female and male baboons are shown in Fig. S2. When baboons were divided into quintiles of FPG levels, a progressive increase in both relative amyloid volume and relative amyloid area was observed (both $P < 0.001$) (Fig. 2 *A* and *B*). There was a strong positive correlation between FPG concentrations and IA severity ($r = 0.662$, $P < 0.001$). Accordingly, the relative islet area free of amyloid showed a linear inverse correlation with FPG levels (Fig. 2*C*) ($P < 0.001$). Abnormal FPG levels were observed in the 2 top quintiles of IA severity (see Table 1); however, overt hyperglycemia was already present during the last 3 years of life only in baboons with the greatest IA severity (Fig. 2*D*, and Table S2). HbA1c levels correlated positively with the relative amyloid area ($r = 0.726$, $P < 0.001$). Fasting plasma glucagon levels increased in the upper 3 quintiles of FPG, and adipose tissue insulin (fasting plasma insulin or FPI) resistance index (FFA × FPI) increased also in these groups (Fig. 2 *E* and *F*) ($P < 0.05$). In Fig. 2 *G* to *L*, representative pancreatic islet from baboons with different degrees of IA are shown. In univariate analysis, age, gender, body weight at the age of 15 years, fasting plasma FFA, insulin, and glucagon levels were all positively correlated with FPG levels (all $P < 0.05$). Multivariate analysis showed that only age (partial $r = -0.20$ $P = 0.03$), gender (partial $r = -0.19$, $P = 0.03$), fasting FFA (partial $r = 0.40$, $P < 0.00013$), and IA (partial $r = 0.65$, $P < 0.0001$) remained significantly correlated with the FPG levels, accounting for the 59% of the total variability. Receiver operating characteristic (ROC) analysis showed that FPG of 90 mg/dL predicted amyloid deposits in more than 25% of the total islet area, with a sensitivity of 74% and a specificity of 83%. For an IA >40%, the same glucose levels had a sensitivity of 84% and a specificity of 77%. At lower and greater levels of IA severity, different FPG levels were equally sensitive and specific in predicting the % of IA (Fig. S3).

**Relationship Between IA Severity and Physical Parameters.** There was a positive correlation between IA severity and age ($r = 0.330$, $P < 0.001$), which persisted after adjusting for gender, and between IA severity and weight at 15 years of age, but only in females ($r = 0.509$, $P < 0.001$), as females with the higher IA severity showed the higher body weight during their entire life (Fig. S4 *A* and *B*, and see Table S2). In both sexes, relative amyloid area increased linearly with the FPG levels (Fig. S4*C*) ($P < 0.001$). At any given FPG level, the severity of IA was slightly higher in overweight baboons, reaching

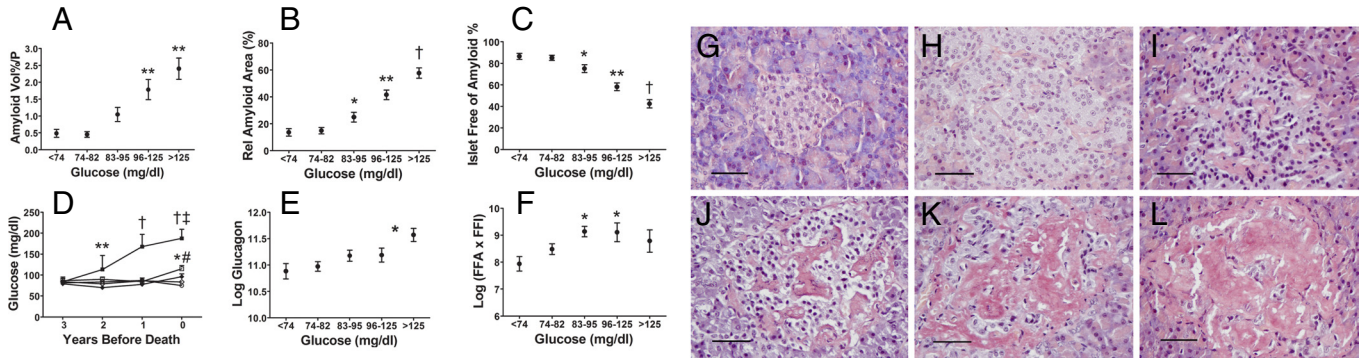


**Fig. 2.** FPG are associated to amyloid deposits, glucagon, and insulin resistance in the adipose tissue, and increases progressively during time in baboons with more severe IA. Relationship between FPG and (*A*) relative amyloid volume/pancreas; (*B*) relative amyloid area; (*C*) islet area free of amyloid; (*D*) glucose levels during the last 4 years of baboon's life according to the degree of amyloid severity at death (open circles Group 1, open diamonds Group 2, filled diamonds Group 3, open squares Group 4, and filled squares Group 5); (*E*) Glucagon levels; and (*F*) Adipose tissue insulin resistance index (fasting FFA × FPI). *, $P < 0.05$ vs. Group 1 and 2; **, $P < 0.05$ vs. G1, 2, and 3; †, $P < 0.05$ vs. all groups; #, $P < 0.05$ vs. glucose 1 year before death (in the same amyloid group); ‡, $P < 0.05$ vs. glucose 3 years before death (in the same amyloid group). (*G–L*) Congo red staining (40×) in pancreas of baboons with different levels of FPG and IA (FPG for *G* = 76, *H* = 80, *I* = 109, *J* = 199, *K* = 195, *L* = 255 mg/dL). (Bar = 50 μm.)

statistical significance in those with FPG between 95 and 125 mg/dL ($P < 0.05$) (Fig. S4*D*).

**Relationship Between IA Severity, Endocrine Cell Replication and Apoptosis, and Relative β- and α-Cell Volume.** The percentage of endocrine islet cells stained for Ki67 correlated with ln(FFA) ($r = 0.480$, $P = 0.037$), total cholesterol ($r = 0.702$, $P < 0.001$), and ln(glucagon) ($r = 0.562$, $P = 0.015$). Because of the smaller number of baboons used for these particular experiments ($n = 20$), results were divided into 3 groups of IA severity, IA of 0 ($n = 4$), 1 to 50 ($n = 8$), and >50% ($n = 8$). Together with the increase in IA severity, there was a progressive, although not significant, increase in the percentage of islet cells undergoing both proliferation (Ki67 positive) and apoptosis (M30 positive) (Fig. 3 *A* and *B*). The difference between proliferation and apoptosis (proliferation-apoptosis = % Ki67-positive − % M30-positive) remained relatively stable with a slight trend to apoptosis (Fig. 3*C*), but the relation between proliferation and apoptosis (proliferation/apoptosis = % Ki67-positive/% M30-positive) was greater in the baboons with IA >50% (Fig. 3*D*) ($P < 0.05$). However, when the cases without IA (IA severity = 0) were compared to those with any degree of IA (IA severity 1–50 + IA severity >50%), proliferation rate was significantly higher in the latter group ($P = <0.05$). Interestingly, we found that in baboons with IA >50% and hyperglycemia, the marker of proliferation (Ki67) colocalized with a fraction of glucagon-positive cells (Fig. 3 *E*, *I*, and *M*) but not with insulin-positive cells (Fig. 3 *F*, *J*, and *N*). This result was confirmed by triple immunofluorescence experiments (Fig. 3 *Q* and *R*): Ki67 staining (green) was detected in the nuclei of a fraction of glucagon-secreting cells only (blue). Conversely, the marker of apoptosis (M30) never colocalized with glucagon-positive cells (Fig. 3 *G*, *K*, and *O*), and colocalized exclusively with insulin-positive cells (Fig. 3 *H*, *L*, and *P*). The relative β-cell volume decreased by >70% in IA >50% (Fig. 4*A*) ($P < 0.001$) and the relative α-cell volume increased by ≈50% in IA >50% and FPG >100 mg/dL (Fig. 4 *B* and *C*) ($P < 0.001$). Number of α cells/total islet cells, number of α cells/islet and individual α-cell size were increased according to IA severity (Fig. 4 *D–F*) ($P < 0.05$) and according to FPG (Fig. S5) ($P < 0.05$).

Electron microscopy revealed amyloid deposits in both the cytoplasm of β cells and in extracellular spaces, with the latter appearing more compact (Fig. S6*A*). Electron microscopy immunocytochemistry demonstrated that both intra- and extracellular deposits were composed of IAPP (Fig. S6 *B* and *C*). The Congo red stain and IAPP immunohistochemistry performed in consecutive pancreatic sections of diabetic baboons also confirmed that the islet amyloid is composed of IAPP (Fig. S7).

**Predictive Model of IA Severity.** We used a multivariate and stratified matched approach to develop a predictive model of amyloid deposition using the following variables: age, gender, overweight at 15 years, FFA, FPG, and insulin and glucagon levels. In a stepwise analysis (Table S3), age and FPG were the best predictors of IA severity, with an adjusted $R^2$ of 0.535 ($P < 0.0001$). In a second model including the 2 strongest predictors of IA severity, age and FPG, the adjusted $R^2$ was 0.519 ($P < 0.0001$). This allowed us to generate the following equation to predict IA severity: Relative amyloid area = 1.118 × Age (years) + 37.57 × FPG (mg/dL) − 164.03. In a stratified analysis, the relationship between IA severity and FPG persisted after matching baboons by age, sex, and weight.

## Discussion

Similar to humans, baboons spontaneously develop insulin resistance associated with obesity and T2DM, thereby serving as a model for the study of the molecular pathogenesis of these conditions (1–4, 28–32). The baboon genome sequencing is underway, but given the high genetic and biologic similarities between humans and nonhuman primates, it is likely that the influence of the genetic background to T2DM is very similar between baboons and humans (28, 32–35). In this study, we demonstrate that the amino acid sequence of baboon IAPP has 92% homology with that of humans, minimal amino acid changes in the amyloidogenic portion, and almost identical predicted fibrillation propensities (see Fig. S1). To assess the role of IA in T2DM, we performed a quantitative morphometric study to evaluate the relationship between IA and islet of Langerhans remodeling in a large number of baboons.

Surprisingly, IA was observed in a large number of baboons with normal FPG levels and in most of those with impaired fasting glucose or T2DM, as defined by using the same cut-off values used for humans (36). A positive correlation between IA and FPG has been reported in transgenic rodents and in vitro but not in humans with T2DM (10, 37–39). In the present study, in which the entire spectrum of FPG was examined, we found a highly significant correlation between IA and both FPG and HbA1c levels. Furthermore, using ROC analysis, we showed that FPG concentrations between 90 and 110 mg/dL have a high predictive value for the presence of worsening IA (see Fig. S3). Thus, these data suggest

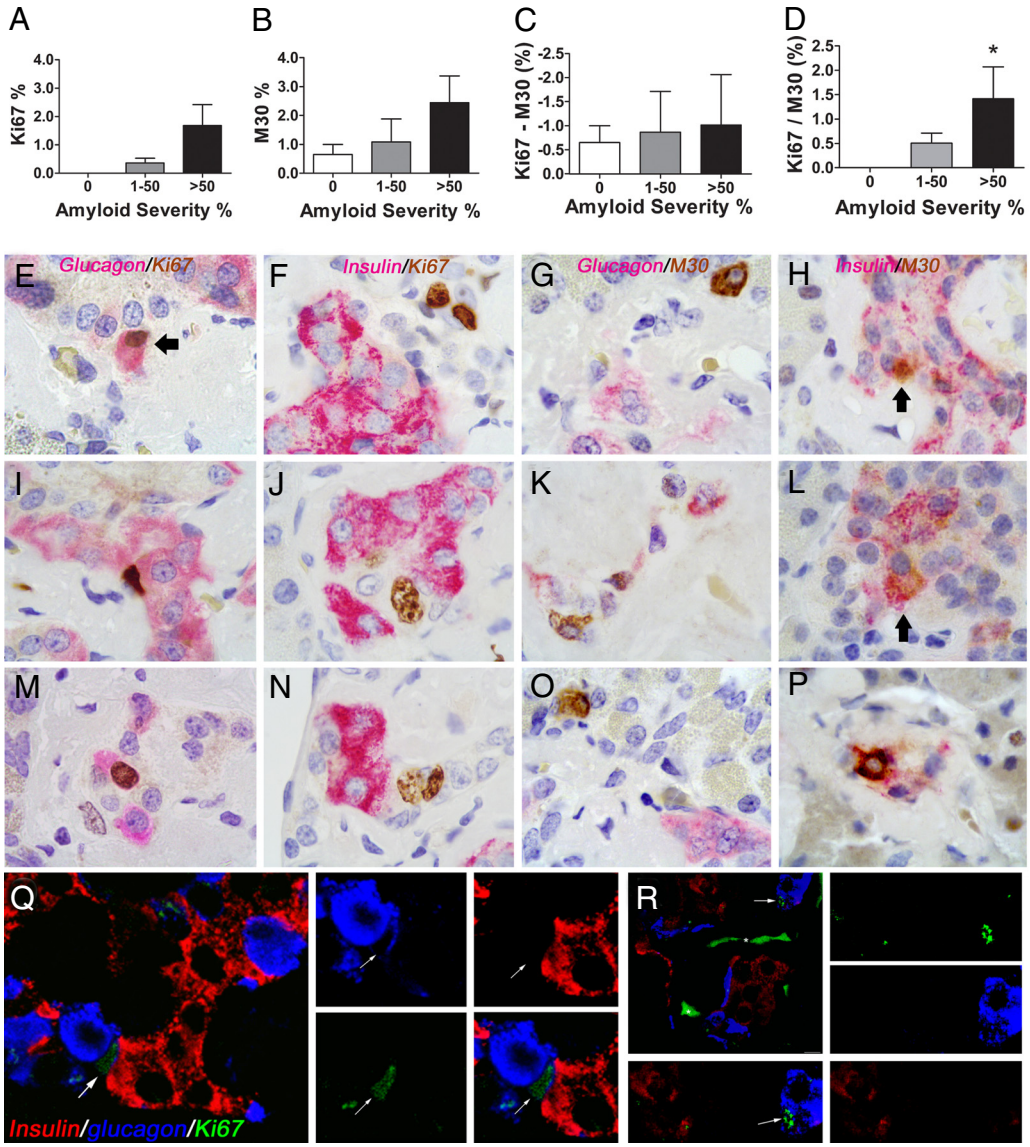


**Fig. 3.** IA severity is associated to β-cell apoptosis and α-cell proliferation. Percentage of endocrine islet cells in proliferation (Ki67) (*A*), apoptosis (M30) (*B*), the difference between these 2 (*C*), and the proliferation/apoptosis ratio (*D*) according to amyloid severity. *$P < 0.05$ vs. control group. Double-label immunohistochemical stains in 3 baboon pancreases with >50% of IA and hyperglycemia show that nuclear immunoreactivity of the proliferative marker Ki67 does colocalize with glucagon in some α cells (*arrow* in *E*; *I*, and *M*), but not with insulin in β cells (*F*, *J*, and *N*). Conversely, cytoplasmic immunoreactivity for the apoptotic marker M30, which detects the caspase cleavage product of cytokeratin 18, does not colocalize with glucagon (*G*, *K*, and *O*), but it does with insulin (*arrows* in *H* and *L*; *P*). Ki67 and M30 are stained in brown, while hormones are stained in red. Triple immunofluorescence staining (*I* and *J*) with Ki67 (*green*), insulin (*red*), and glucagon (*blue*) confirming that nuclear staining of the proliferative marker Ki67 was detected in few glucagon-positive cells (*blue*, *arrows*), but not in insulin-positive β cells (*red*). A particular at higher magnification (2×) is shown. *, Amyloid deposits autofluorescence. (Scale bar, 10 μm.)

that IA plays an important pathogenic role in the development of β-cell dysfunction in baboons and humans.

In the baboons with the most extensive IA, FPG concentrations increased progressively during the last 3 years of life, while in baboons in the fourth quintile of IA severity, FPG concentrations increased in the last year, suggesting that progression from normoglycemia/little-or-no IA to hyperglycemia/extensive IA occurs in the last 3 years (see Fig. 2D). We also found a hyperbolic relationship ($r = 0.942$ $P < 0.001$) (see Fig. S1) between IA severity and IA prevalence, as previously reported in humans and mice (40, 41). However, in contrast to what is observed in rodents, amyloid deposition in baboons seems to occur in 3 phases. The first phase is marked by a large increase in amyloid prevalence (from 0 to 50%) but only a small increase in amyloid severity (from 0 to 9.5%, $P$ = NS). In contrast, amyloid severity increases dramatically in the second phase (from 9.5% to 47.3%, $P < 0.001$) and a further increase in amyloid prevalence (from 50 to 95%, $P < 0.001$) is noted. Finally, in the third phase, amyloid severity increases further in each individual islet (from 47.3 ± to 68.9%, $P < 0.001$), with negligible changes in amyloid prevalence (from 95 to 100%, $P$ = NS).

Similarly to what occurs in humans, hyperglycemia was paralleled by increased insulin resistance and decreased β-cell function. Moreover, hyperglycemia and IA produced an additive negative effect on β-cell function (see Fig. 1) (1, 4, 5). The relationship between IA severity and FPI concentrations was that of an inverted U-shaped curve consistent with previous reports in humans and nonhuman primates during the progression from normal glucose tolerance to T2DM (1, 20, 26, 27, 42).

Using a multivariate analysis, we found that increased FFA concentrations and the increased magnitude of IA were the most

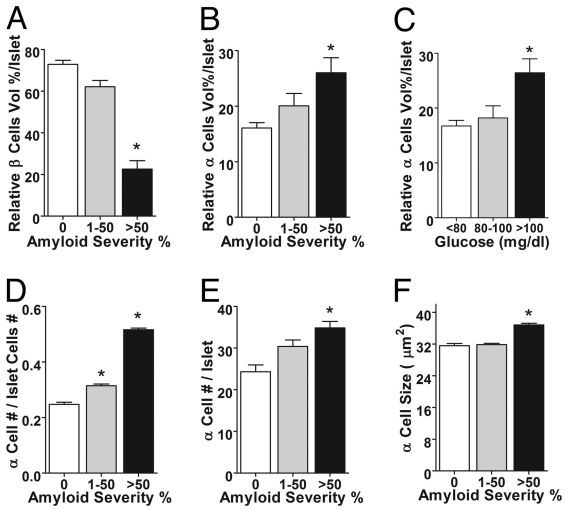


**Fig. 4.** IA is associated with a reduction in the relative $\beta$-cell volume and an increase in the relative $\alpha$-cell volume depending on $\alpha$-cell proliferation and hypertrophy. Relative $\beta$- and $\alpha$-cell volume (*A* and *B*) according to amyloid severity; relative $\alpha$-cell volume according to FPG (*C*); $\alpha$-cell number/total islet cell number (*D*), absolute $\alpha$-cell number/islet (*E*), and $\alpha$-cell size (*F*) according to amyloid severity. *, $P < 0.05$ vs. control group.

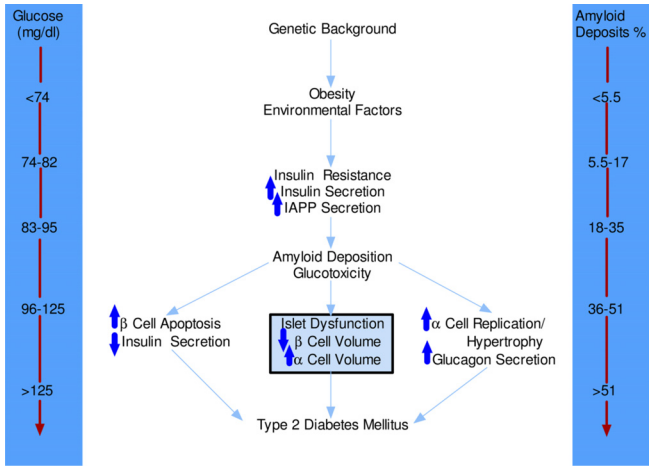


**Fig. 5.** Proposed natural history of the events leading to the progression from normal glucose tolerance to T2DM in baboons.

important determinants of fasting hyperglycemia. Both insulin resistance and the incidence of T2DM increase with age, and in our baboon population aging was positively correlated with IA (42). Multivariate analysis identified age and FPG as the best predictors of IA severity, thereby allowing us to generate a equation to predict IA severity.

Amyloid deposition has been associated with $\beta$-cell apoptosis, both in vivo and in vitro (21, 23, 24, 43, 44). Surprisingly, with the increase in the severity of IA, we found an increased rate of both replication and apoptosis in the islet cells (see Fig. 3 *A* and *B*). The increase in islet-cell apoptosis was limited to $\beta$ cells, while the increase in islet-cell replication was exclusively pertinent to $\alpha$ cells (see Fig. 3 *E*–*R*). Therefore, progressive IA is associated not only with increased $\beta$-cell apoptosis (reduced relative $\beta$-cell volume) but also with increased $\alpha$-cell replication and hypertrophy (increased relative $\alpha$-cell volume). Although reduced $\beta$-cell volume, increased $\alpha$-cell volume, and relative or absolute hyperglucagonemia have been reported previously, $\alpha$-cell proliferation and hypertrophy have not been reported previously in nonhuman primates or in humans with T2DM, to our knowledge, and could represent a plausible biological explanation for hyperglucagonemia (6, 20, 45–47).

In conclusion, we propose that in the presence of a predisposing genetic background, the combination of environmental factors (high-fat diet and obesity) may precipitate insulin resistance with an over-stimulation of $\beta$ cells to over-secrete insulin to maintain normoglycemia. Concurrent with hyperinsulinemia, increased IAPP secretion and the beginning of IAPP deposition (both intracellularly and extracellularly) occurs. Whether IA is a cause or consequence of $\beta$-cell dysfunction/hyperglycemia is controversial, but we believe that IA plays a causative role in the $\beta$-cell dysfunction/apoptosis that is observed in T2DM in a manner that is similar to other human diseases that are associated with amyloid deposits, causing dysfunction of the affected tissue and organs (18, 20, 21, 23–25, 27, 43, 45, 48–50). In this context, $\alpha$-cell proliferation and hypertrophy occurs, leading to an imbalance in the $\alpha$-/$\beta$-cell ratio (islet of Langerhans dysfunctional remodeling) and the onset of overt T2DM (Fig. 5). Further studies will aim to understand the molecular mechanisms of these phenomena and novel treatments based on them.

## Materials and Methods

Methods for sequencing of baboon IAPP, determining its predicted fibrillogenic propensities, and immunofluorescence staining are described in *SI Materials and Methods*.

**Baboons.** We examined retrospectively all necropsies performed in baboons over the last 15 years (from 1994 to 2008) at the Southwest National Primate Research Center at the Southwest Foundation for Biomedical Research at San Antonio. All animals had been fed standard chow diet 5038 (Purina) and received water ad libitum. All animals in this report were cared for in compliance with the Guide for the Care of Laboratory Animals. All procedures were approved by the SFBR Institutional Animal Care and Use Committee. The SFBR is accredited by the Association for Assessment and Accreditation of Laboratory Animal Care, International. Out of the 2,254 screened baboons, 150 met the following eligibility criteria: (*i*) age >8 years, (*ii*) availability of pancreatic tissue, and (*iii*) availability of anthropometric and laboratory data. Exclusion criteria were (*i*) presence of extrapancreatic amyloidosis and (*ii*) participation in experimental protocols that could theoretically affect pancreatic amyloid deposition.

Baboons were considered overweight (>21.7 and >33.6 kg in females and males, respectively) when above the 75th percentile of a body weight distribution (see Fig. S2 *A* and *B*). Normal FPG values (80 ± 1.2 and 79 ± 1.3 mg/dL in females and males, respectively) were identified by measuring FPG in 452 healthy adult baboons (see Fig. S2 *C* and *D*). The selected 150 baboons were divided into quintiles according to the FPG and IA.

**Analytical Measurements and Metabolic Parameters.** FPG, HbA1c, insulin, glucagon, FFA, insulin secretion index (HOMA-$\beta$), insulin resistance index (HOMA-IR), and adipose tissue insulin resistance were measured as described in *SI Materials and Methods*.

**Histology and Immunohistochemistry.** All of the 150 pancreases were fixed in 10% neutral-buffered formalin and paraffin embedded. Sections 5-$\mu$m thick were stained with H&E and with Congo red. For immunohistochemistry, after endogenous peroxidase activity inhibition, 3-$\mu$m-thick sections were incubated with the primary antibody at 4 °C for 18 to 20 h, followed by the avidin–biotin complex procedure (51). Immunoreactions were developed using 0.03% 3,3′-diaminobenzidine tetrahydrochloride. The following antibodies were used: anti-insulin mouse monoclonal (clone AE9D6, Biogenex Laboratories), anti-glucagon rabbit polyclonal (Milab), anti-caspase cleavage product of cytokeratin 18 mouse monoclonal (clone M30, Hoffmann-LaRoche), and anti-Ki67 mouse monoclonal (clone MIB1, Dako). Colocalization studies were performed using double-label immunohistochemical stains (52). Ki67- and M30-positive cells were counted in a subgroup of 20 pancreases that were divided into 3 groups according to the severity of islet amyloidosis and were expressed as the percentage of positive cells over total counted islet cells (with a minimum of 500 counted cells). The observers (C. Placidi, G.F., and S.L.R.) were blind to the severity of islet amyloidosis at the time of the quantification of proliferating or apoptotic cells.

**Morphometric Analysis.** Morphometric analysis was performed using the Computer Assisted Stereology Toolbox (CAST) 2.0 system from Olympus and using

the stereology fundamentals that allowed us to calculate the area and volume of the different microscopic structures through the use of lines and points. In this way, IA was expressed as the percentage of islet area occupied by amyloid deposits (relative amyloid area), and the relative volume of $\beta$ and $\alpha$ cells as the percentage of islet volume occupied by these specific endocrine cells; $\alpha$-cell size and number were also measured (see *SI Materials and Methods*).

**Statistical Analysis.** Data are presented as mean ± SEM. Variables with a skewed distribution were log transformed. ANOVA was used for comparisons between more than 2 groups with a Bonferroni as a post hoc test. Pearson's correlation coefficient was used to evaluate correlations between variables. ROC analysis was used to examine the sensitivity, specificity, and predictive values of different glucose levels to estimate IA severity. Regression analysis was performed to evaluate the impact of different variables on FPG and IA severity. A $P < 0.05$ was considered statistically significant.

**ACKNOWLEDGMENTS.** We thank Iram P. Rodriguez-Sanchez for technical help in the sequencing of IAPP, Dr. David Eisenberg (Howard Hughes Institute and University of California at Los Angeles) for critical discussion, and Dr. Leslie David Hillis for enthusiastic support and critical reading of the manuscript. This work was supported by start-up funds from the University of Texas Health Science Center (F.F.). R.G.-M. was supported by a Ralph A. DeFronzo Postdoctoral Fellowship from Mexican Endocrine Society/Sanofi-Aventis and the Consejo Nacional de Ciencia y Tecnologia (CONACYT, Mexico). This work is part of the PhD requirements for R.G.-M. at the University of Colima, Mexico, and was partially supported by the National Institutes of Health/National Center for Research Resources Grant P51 RR013986 to the Southwest National Primate Center; the investigation was conducted in part in facilities constructed with support from the Research Facilities Improvement Program under Grant numbers C06 RR014578, C06 RR013556, C06 RR015456, C06 RR017515 (to G.B.H., E.J.D., A.G.C.). J.H. was supported by Robert A. Welch Foundation Grant AQ-1399.

1. Gastaldelli A, Ferrannini E, Miyazaki Y, Matsuda M, DeFronzo RA (2004) Beta-cell dysfunction and glucose intolerance: results from the San Antonio metabolism (SAM) study. *Diabetologia* 47:31–39.
2. Taniguchi CM, Emanuelli B, Kahn CR (2006) Critical nodes in signalling pathways: insights into insulin action. *Nat Rev* Mol Cell Biol 7:85–96.
3. Biddinger SB, Kahn CR (2006) From mice to men: insights into the insulin resistance syndromes. *Annu Rev Physiol* 68:123–158.
4. Weir GC, Bonner-Weir S (2004) Five stages of evolving beta-cell dysfunction during progression to diabetes. *Diabetes 53 Suppl* 3:S16–S21.
5. Federici M, et al. (2001) High glucose causes apoptosis in cultured human pancreatic islets of Langerhans: a potential role for regulation of specific Bcl family genes toward an apoptotic cell death program. *Diabetes* 50:1290–1301.
6. Butler AE, et al. (2003) Beta-cell deficit and increased beta-cell apoptosis in humans with type 2 diabetes. *Diabetes* 52:102–110.
7. Clark A, et al. (1990) Islet amyloid polypeptide in diabetic and non-diabetic Pima Indians. *Diabetologia* 33:285–289.
8. Rocken C, Linke RP, Saeger W (1992) Immunohistology of islet amyloid polypeptide in diabetes mellitus: semi-quantitative studies in a post-mortem series. *Virchows Arch A Pathol Anat Histopathol* 421:339–344.
9. Sempoux C, Guiot Y, Dubois D, Moulin P, Rahier J (2001) Human type 2 diabetes: morphological evidence for abnormal beta-cell function. *Diabetes 50 Suppl* 1:S172–S177.
10. Zhao HL, et al. (2003) Prevalence and clinicopathological characteristics of islet amyloid in Chinese patients with type 2 diabetes. *Diabetes* 52:2759–2766.
11. Hoppener JW, Ahren B, Lips CJ (2000) Islet amyloid and type 2 diabetes mellitus. *N Engl J Med* 343:411–419.
12. Cooper GJ, et al. (1987) Purification and characterization of a peptide from amyloid-rich pancreases of type 2 diabetic patients. *Proc Natl Acad Sci USA* 84:8628–8632.
13. Westermark P, Wernstedt C, O'Brien TD, Hayden DW, Johnson KH (1987) Islet amyloid in type 2 human diabetes mellitus and adult diabetic cats contains a novel putative polypeptide hormone. *Am J Pathol* 127:414–417.
14. Hou X, et al. (1999) Prolonged exposure of pancreatic beta cells to raised glucose concentrations results in increased cellular content of islet amyloid polypeptide precursors. *Diabetologia* 42:188–194.
15. Marzban L, et al. (2006) Impaired NH2-terminal processing of human proislet amyloid polypeptide by the prohormone convertase PC2 leads to amyloid formation and cell death. *Diabetes* 55:2192–2201.
16. Westermark P, Li ZC, Westermark GT, Leckstrom A, Steiner DF (1996) Effects of beta cell granule components on human islet amyloid polypeptide fibril formation. *FEBS Lett* 379:203–206.
17. Paulsson JF, Westermark GT (2005) Aberrant processing of human proislet amyloid polypeptide results in increased amyloid formation. *Diabetes* 54:2117–2125.
18. Westermark GT, Westermark P, Berne C, Korsgren O (2008) Widespread amyloid deposition in transplanted human pancreatic islets. *N Engl J Med* 359:977–979.
19. Davalli AM, et al. (2008) Disproportionate hyperproinsulinemia, beta-cell restricted prohormone convertase 2 deficiency, and cell cycle inhibitors expression by human islets transplanted into athymic nude mice: insights into nonimmune-mediated mechanisms of delayed islet graft failure. *Cell Transplant* 17:1323–1336.
20. Clark A, et al. (1988) Islet amyloid, increased A-cells, reduced B-cells and exocrine fibrosis: quantitative changes in the pancreas in type 2 diabetes. *Diabetes Res* 9:151–159.
21. Huang CJ, et al. (2007) High expression rates of human islet amyloid polypeptide induce endoplasmic reticulum stress mediated beta-cell apoptosis, a characteristic of humans with type 2 but not type 1 diabetes. *Diabetes* 56:2016–2027.
22. Lorenzo A, Razzaboni B, Weir GC, Yankner BA (1994) Pancreatic islet cell toxicity of amylin associated with type-2 diabetes mellitus. *Nature* 368:756–760.
23. Mirzabekov TA, Lin MC, Kagan BL (1996) Pore formation by the cytotoxic islet amyloid polypeptide amylin. *J Biol Chem* 271:1988–1992.
24. Ritzel RA, Meier JJ, Lin CY, Veldhuis JD, Butler PC (2007) Human islet amyloid polypeptide oligomers disrupt cell coupling, induce apoptosis, and impair insulin secretion in isolated human islets. *Diabetes* 56:65–71.
25. Westermark P, Wilander E (1978) The influence of amyloid deposits on the islet volume in maturity onset diabetes mellitus. *Diabetologia* 15:417–421.
26. Howard CF, Jr. (1986) Longitudinal studies on the development of diabetes in individual *Macaca nigra*. *Diabetologia* 29:301–306.
27. de Koning EJ, Bodkin NL, Hansen BC, Clark A (1993) Diabetes mellitus in *Macaca mulatta* monkeys is characterised by islet amyloidosis and reduction in beta-cell population. *Diabetologia* 36:378–384.
28. Chavez AO, et al. (2008) Physiological and molecular determinants of insulin action in the baboon. *Diabetes* 57:899–908.
29. DeFronzo RA, Bonadonna RC, Ferrannini E (1992) Pathogenesis of NIDDM. A balanced overview. *Diabetes Care* 15:318–368.
30. Hubbard GB, Steele KE, Davis KJ, 3rd, Leland MM (2002) Spontaneous pancreatic islet amyloidosis in 40 baboons. *J Med Primatol* 31:84–90.
31. Stokes WS (1986) Spontaneous diabetes mellitus in a baboon (*Papio cynocephalus anubis*). *Lab Anim Sci* 36:529–533.
32. Comuzzie AG, et al. (2003) The baboon as a nonhuman primate model for the study of the genetics of obesity. *Obes Res* 11:75–80.
33. Gibbs RA, et al. (2007) Evolutionary and biomedical insights from the rhesus macaque genome. *Science* 316:222–234.
34. Anonymous (2005) Initial sequence of the chimpanzee genome and comparison with the human genome. *Nature* 437:69–87.
35. Chavez AO, et al. (2009) Predictive models of insulin resistance derived from simple morphometric and biochemical indices related to obesity and the metabolic syndrome in baboons. *Cardiovasc Diabetol* 8:22–30..
36. Anonymous (2008) Diagnosis and classification of diabetes mellitus. *Diabetes Care 31 Suppl* 1:S55–S60.
37. Hayden MR, et al. (2007) Longitudinal ultrastructure study of islet amyloid in the HIP rat model of type 2 diabetes mellitus. *Exp Biol Med (Maywood)* 232:772–779.
38. Verchere CB, et al. (1996) Islet amyloid formation associated with hyperglycemia in transgenic mice with pancreatic beta cell expression of human islet amyloid polypeptide. *Proc Natl Acad Sci USA* 93:3492–3496.
39. Zraika S, et al. (2007) Glucose- and time-dependence of islet amyloid formation in vitro. *Biochem Biophys Res Commun* 354:234–239.
40. Wang F, Hull RL, Vidal J, Cnop M, Kahn SE (2001) Islet amyloid develops diffusely throughout the pancreas before becoming severe and replacing endocrine cells. *Diabetes* 50:2514–2520.
41. Westermark P (1972) Quantitative studies on amyloid in the islets of Langerhans. *Ups J Med Sci* 77:91–94.
42. Martin BC, et al. (1992) Role of glucose and insulin resistance in development of type 2 diabetes mellitus: results of a 25-year follow-up study. *Lancet* 340:925–929.
43. Matveyenko AV, Gurlo T, Daval M, Butler AE, Butler PC (2009) Successful versus failed adaptation to high-fat diet-induced insulin resistance: the role of IAPP-induced beta-cell endoplasmic reticulum stress. *Diabetes* 58:906–916.
44. Paulsson JF, Andersson A, Westermark P, Westermark GT (2006) Intracellular amyloid-like deposits contain unprocessed pro-islet amyloid polypeptide (proIAPP) in beta cells of transgenic mice overexpressing the gene for human IAPP and transplanted human islets. *Diabetologia* 49:1237–1246.
45. Yoon KH, et al. (2003) Selective beta-cell loss and alpha-cell expansion in patients with type 2 diabetes mellitus in Korea. *J Clin Endocrinol Metab* 88:2300–2308.
46. Iki K, Pour PM (2007) Distribution of pancreatic endocrine cells including IAPP-expressing cells in non-diabetic and type 2 diabetic cases. *J Histochem Cytochem* 55:111–118.
47. Dunning BE, Gerich JE (2007) The role of alpha-cell dysregulation in fasting and postprandial hyperglycemia in type 2 diabetes and therapeutic implications. *Endocr Rev* 28:253–283.
48. Janson J, Ashley RH, Harrison D, McIntyre S, Butler PC (1999) The mechanism of islet amyloid polypeptide toxicity is membrane disruption by intermediate-sized toxic amyloid particles. *Diabetes* 48:491–498.
49. Chiti F, Dobson CM (2006) Protein misfolding, functional amyloid, and human disease. *Annu Rev Biochem* 75:333–366.
50. Westermark P (2005) Aspects on human amyloid forms and their fibril polypeptides. *FEBS J* 272:5942–5949.
51. Hsu SM, Raine L, Fanger H (1981) Use of avidin-biotin-peroxidase complex (ABC) in immunoperoxidase techniques: a comparison between ABC and unlabeled antibody (PAP) procedures. *J Histochem Cytochem* 29:577–580.
52. Lan HY, Mu W, Nikolic-Paterson DJ, Atkins RC (1995) A novel, simple, reliable, and sensitive method for multiple immunoenzyme staining: use of microwave oven heating to block antibody crossreactivity and retrieve antigens. *J Histochem Cytochem* 43:97–102.